Optimal operating points of PEM fuel cell model with RSM [†]

Dongji Xuan, Zhenzhe Li, Jinwan Kim and Youngbae Kim[*]

Department of Mechanical Engineering, Chonnam National University,
300 Yongbong-dong, Buk-gu, Gwangju 500-757, Korea

Abstract

The output power efficiency of the fuel cell system mainly depends on the required current, stack temperature, air excess ratio, hydrogen excess ratio, and inlet air humidity. Therefore, the operating conditions should be optimized to get maximum output power efficiency. In this paper, a dynamic model for the fuel cell stack was developed, which is comprised of a mass flow model, a gas diffusion layer model, a membrane hydration, and a stack voltage model. Experiments have been performed to calibrate the dynamic Polymer Electrolyte Membrane Fuel Cell (PEMFC) stack model. To achieve the maximum output power and the minimum use of hydrogen in a certain power condition, optimization was carried out using Response Surface Methodology (RSM) based on the proposed PEMFC stack model. Using the developed method, optimal operating conditions can be effectively selected in order to obtain minimum hydrogen consumption.

Keywords: Dynamic modeling; Gas diffusion layer; Optimization; PEMFC; RSM

---

1. Introduction

With the heightened concern for energy consumption and environment conservation, the need for alternative energy sources has also greatly increased. Compared with other alternative energy sources such as wind power, solar energy, and tidal energy, the fuel cell, which uses hydrogen energy, has been more adverted to because of its environmental friendliness, high efficiency, low noise, and low vibration. Recently, Polymer Electrolyte Membrane Fuel Cell (PEMFC) has been widely studied for its use as a power source in automobiles or small-sized generators due to its comparable low power output, low operating temperature, high efficiency, high current density, and structural safety compared with other fuel cell systems [1]. However, to fully commercialize this technique, it is still necessary to maximize its operating power and

minimize the cost. Many research works have been done to achieve these objectives, but it is not easy to attain them because the PEMFC variables are closely interdependent, which also results in trouble for the optimization of the PEMFC variables. To achieve optimization for the fuel cell, an exact performance prediction is required with various operating variables involved in the fuel cell system.

The modeling for PEMFC was first presented in the 1990s, and a number of studies have been published since then. For instance, Verbrugge and Hill made the fuel cell model to strengthen the polymer electrolyte membrane [2]. Bernardi et al. and Springer et al. introduced the sandwich model using a cathode, an anode, and a membrane [3, 4]. Based on the sandwich model, the mathematical modeling for the fuel cell has been addressed and then followed by its computational simulation.

Among the research conducted in the 21st century are those by Sylvain et al., who analyzed high and low pressure system characteristics using the dynamic model [5], and Pukrushpan et al., who made the state

space dynamic model for control purpose [6]. However, these dynamic modeling are highly complex because of their interrelated mathematical expressions, which makes it difficult to perform the optimization.

Most fuel cell models have not clearly discussed the gas diffusion layer (GDL)−a two-phase flow model. Nam was the first to address the GDL with a one-dimensional partial differential equation form, but it is cumbersome to solve the equation using an iterative technique [7]. Based on Nam's model, numerous studies have turned to the two-phase (water and vapor) flow at the anode and cathode layers. Among them are those by McKay, Del Real, and Park, in which Nam's model was incorporated into the PEMFC models [8-10]. The solution is also an iterative one, so the optimal operating solution is difficult to obtain using these models.

Recently, optimal operating studies for the PEMFC have been performed. For instance, Park used the equivalent fuel efficiency algorithm to obtain the optimal operating conditions of the PEMFC in the Federal Urban Driving Schedule mode [11]. Kim used stochastic dynamic programming to obtain the optimal fuel cell numbers [12]. Sikha performed the PEMFC with a battery-capacitor system to obtain the optimal operating solution using the variables duty ratio, pulse frequency ratio, and capacitor configuration index [13]. However, a detailed PEMFC model was lacking in their work. Lin et al. performed the PEMFC optimization using the simple conjugate-gradient method [14]. Their primary objective was to obtain the optimal design parameters of the PEMFC rather than the operating parameters. The design parameters were channel width ratio, porosity of GDL, and porosity of the catalyst layer. Their results gave the optimized design parameters for the maximum power of the PEMFC system, but the partial differential equations with boundary condition and initial condition were omitted.

Therefore, in this study, we tried to obtain the optimal operating conditions using a PEMFC model. To apply this method as easily as possible, one-dimensional differential equations were derived including GDL. Response Surface Methodology (RSM) is then used to achieve the best performance employing highly interrelated variables [15]. In using RSM, optimization of the operating variables can be achieved more easily with less computational effort [16, 17].

The organization of this paper is as follows: dyna-

mic modeling of PEMFC using a simple GDL model is introduced in Chapter 2, experiments are performed to calibrate the dynamic model in Chapter 3, then the Sequential Quadratic Programming (SQP) optimization algorithm [18] is applied in Chapter 4 for fuel cell power optimization and minimum hydrogen consumption condition using a constructed response surface. Finally, the conclusion is presented in Chapter 5.

2. Dynamic model for fuel cell

For future control purposes, a dynamic PEMFC stack model was developed instead of steady-state model. The dynamic model for the fuel cell stack is comprised of six parts as shown in Fig. 1: (1) membrane hydration, (2) cathode mass flow, (3) anode mass flow, (4) stack voltage, (5) cathode GDL, and (6) anode GDL. In this paper, a simplified model was obtained by assuming that the stack temperature is constant. This assumption is justified because the stack temperature changes relatively slowly, compared with the 100ms transient dynamics included in the model to be developed. Additionally, it is also assumed that the temperature is perfectly controlled by cooling systems.
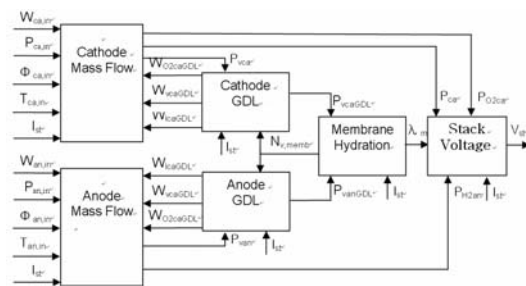
Fig. 1. Fuel cell stack block diagram.

2.1 Cathode mass flow model

The cathode mass flow model is expressed using the ideal gas state equation, mass conservation, and thermodynamic relation for the mixed gas condition. The assumptions below are designed to simplify the model:

(1) The materials, including fuel and air, are compatible with the ideal gas state equation.
(2) The stack temperature is constant and is the same as the internal gas temperature.
(3) The thermodynamic variables (temperature, pressure, and humidity) and chemical compo-

sition of the internal stack are the same as the outlet of the stack.

Oxygen, nitrogen, and water dynamic characteristics inside the cathode can be expressed using the four mass flow conservation equations.

$$\frac{dm_{O_2,ca}}{dt} = W_{O_2,cain} - W_{O_2,caout} - W_{O_2,caGDL} \tag{1}$$

$$\frac{dm_{N_2,ca}}{dt} = W_{N_2,cain} - W_{N_2,caout} \tag{2}$$

$$\frac{dm_{v,ca}}{dt} = W_{v,ca,in} - W_{v,ca,out} + W_{v,caGDL} + W_{ca,evap} \tag{3}$$

$$\frac{dm_{l,ca}}{dt} = W_{l,ca,in} - W_{l,ca,out} - W_{ca,evap} + W_{l,caGDL} \tag{4}$$

where

$$W_{ca,evap} = \min\left(A_{fc}\left(P_{sat}\left(T_{st}\right) - P_{v,ca}\right)\sqrt{\frac{M_v}{2\pi R_v T_{st}}}, W_{l,caGDL} \right) \tag{5}$$

Using the ideal gas state equation, the partial pressure for oxygen, nitrogen, and vapor inside the cathode channel flow can be represented as follows:

$$P_{O_2,ca} = \frac{m_{O_2,ca}R_{O_2}T_{st}}{V_{ca}} \tag{6}$$

$$P_{N_2,ca} = \frac{m_{N_2,ca}R_{N_2}T_{st}}{V_{ca}} \tag{7}$$

$$P_{v,ca} = \frac{m_{v,ca}R_v T_{st}}{V_{ca}} \tag{8}$$

The inlet vapor pressure can be expressed as

$$P_{v,ca,in} = \phi_{ca,in}P_{sat}\left(T_{ca,in}\right) \tag{9}$$

The saturated vapor pressure P_{sat} is represented by the empirical relation as

$$P_{sat}(T) = P_0 \times 10^{2.953\times10^{-2}(T-273.15)-9.1837\times10^{-5}(T-273.15)^2}$$
$$\times 10^{-1.4454\times10^{-7}(T-273.15)^3-2.1794} \tag{10}$$

in which P_0 is the standard atmospheric pressure. The humidity ratio $\omega_{ca,in}$ can be expressed as

$$\omega_{ca,in} = \frac{M_v P_{v,ca,in}}{M_{a,ca,in}P_{a,ca,in}} \tag{11}$$

$$P_{a,ca,in} = P_{ca,in} - P_{v,ca,in} \tag{12}$$

$$M_{a,ca,in} = y_{O_2,ca,in} \times M_{O_2} + (1 - y_{O_2,ca,in}) \times M_{N_2} \tag{13}$$

The mass flow at the cathode inlet materials can be obtained as

$$W_{l,ca,in} = 0 \tag{14}$$

$$W_{a,ca,in} = \frac{1}{1 + w_{ca,in}}W_{ca,in} \tag{15}$$

$$W_{v,ca,in} = W_{ca,in} - W_{a,ca,in} \tag{16}$$

$$W_{O_2,ca,in} = x_{O_2,ca,in}W_{a,ca,in} \tag{17}$$

$$W_{N_2,ca,in} = \left(1 - x_{O_2,ca,in}\right)W_{a,ca,in} \tag{18}$$

$$x_{O_2ca,in} = \frac{y_{O_2;ca,in} \times M_{O_2}}{y_{O_2,ca,in} \times M_{O_2} + (1 - y_{O_2,ca,in}) \times M_{N_2}} \tag{19}$$

The total mass flow at the cathode outlet can be expressed by the equation below [9].

$$W_{ca,out} = K_{ca,out}(P_{ca} - P_{ca,out}) \tag{20}$$

With the above chemical relations and assumption, thermodynamic variables are the same as those in the cathode outlet. Thus, the fuel cell stack outlet mass flow of $W_{O_2,ca,out}$, $W_{N_2,ca,out}$, and $W_{v,ca,out}$ can be calculated using Eq. 9 to Eq. 20, respectively.

2.2 Anode mass flow model

Since the anode mass flow model is quite similar to the cathode model [6], the compact expression of the oxygen, nitrogen, water mass conservation equation at the inside of anode, and the total mass flow equation can be expressed as

$$\frac{dm_{H_2,an}}{dt} = W_{H_2,anin} - W_{H_2,anout} - W_{H2,anGDL} \tag{21}$$

$$\frac{dm_{v,an}}{dt} = W_{v,an,in} - W_{v,ca,out} - W_{v,anGDL} + W_{an,evap} \tag{22}$$

$$\frac{dm_{l,an}}{dt} = W_{l,an,in} - W_{l,an,out} - W_{an,evap} - W_{l,anGDL} \tag{23}$$

$$W_{an,out} = K_{an,out}(P_{an} - P_{atm}) \tag{24}$$

$$W_{l,an,out} = \frac{m_{l,an}}{t_{purge}} \tag{25}$$

2.3 Membrane hydration model

As the content of water (i.e., liquid water and vapor) has a strong effect on ion conductivity, the dynamic model should contain detailed water reaction

characteristics for membrane electrode assembly. According to Nguyen et al., two water molecule delivery models have been studied [4, 19]. The first one is due to osmotic resistance, while the second one is due to the inverse diffusion based on the concentration curvature between two materials.

Combining the two phenomena, water mass flow from anode to cathode can be expressed as

$$W_{v,memb} = M_v A_{fc} n \left(\frac{n_d i}{F} - D_w \frac{c_{v,ca} - c_{v,an}}{t_m} \right) \quad (26)$$

The electro osmotic drag coefficient n_d depends on the membrane water content λ_m and water activity a.

$$c_{v,j} = \frac{\rho_{memb,dry}}{M_{memb,dry}} \lambda_j \quad (27)$$

$$n_d = 0.0029\lambda_m^2 + 0.05\lambda_m - 3.4 \times 10^{-19} \quad (28)$$

$$\lambda_i = \begin{cases} 0.043 + 17.81a - 39.85a^2 + 36a & ,0 < a_i \le 1 \\ 14 + 1.4(a-1) & ,1 \le a_i \le 3 \end{cases} \quad (29)$$

where $\lambda_m = (\lambda_{ca} + \lambda_{an})/2$, the water activity $a_i = p_{v,i}/p_{sat,i}$, and $i \in [ca, \ an]$.

The diffusion coefficient at the electrolyte D_w can be represented by the empirical equation below [20].

$$D_w = D_\lambda \exp\left[2416\left(\frac{1}{303} - \frac{1}{T_{st}} \right) \right] \quad (30)$$

$$D_\lambda = \begin{cases} 10^{-6} & ,\lambda_m < 2 \\ 10^{-6}(1 + 2(\lambda_m - 2)) & ,2 \le \lambda_m < 3 \\ 10^{-6}(3 - 1.67(\lambda_m - 3)) & ,3 \le \lambda_m < 4.5 \\ 1.25 \times 10^{-6} & ,\lambda_m \ge 4.5 \end{cases} \quad (31)$$

2.4 Stack voltage model

Fuel cell stack modeling can be expressed by the term which thermodynamically uses open circuit voltage (OCV), irreversible activity voltage loss, resistance voltage loss, and concentration voltage loss.

$$V_{fc} = E - V_{act} - V_{ohm} - V_{conc} \quad (32)$$

The fuel cell stack OCV can be expressed by the Nernst equation below [21].

$$E = 1.229 - 8.5 \times 10^{-4}(T_{fc} - 298.15) + 4.3085 \times 10^{-5} T_{fc}\left[\ln(P_{H_2}) + 0.5\ln(P_{O_2}) \right] \quad (33)$$

where T_{fc} is the fuel cell operating temperature, and P_{H_2} and P_{O_2} are the partial pressures of hydrogen and oxygen, respectively.

The activity voltage loss v_{act} arises from the need to move electrons and to break and form chemical bonds at the anode and cathode. The relationship between activation overvoltage and current density by the Tafel equation is approximated by [6]

$$V_{act} = v_0 + v_a(1 - e^{-i/c_1}) \quad (34)$$

where v_o, v_a, and c_1 are the constants depending on the cell specification represented in Table 1.

$$v_0 = 0.279 - 8.5 \times 10^{-4}(T_{st} - 298.15) + 4.3085 \times 10^{-5} T_{st} \\ \left[\ln\left(\frac{p_{ca} - p_{sat}}{1.01325} \right) + 0.5\ln\left(\frac{0.1173(p_{ca} - p_{sat})}{1.01325} \right) \right] \quad (35)$$

$$v_a = (-1.618 \times 10^{-5} T_{st} + 1.618 \times 10^{-2})(\frac{p_{O_2}}{0.1173} + p_{sat})^2 + \\ (1.8 \times 10^{-4} T_{st} - 0.166)(\frac{p_{O_2}}{0.1173} + p_{sat}) + \\ (-5.8 \times 10^{-4} T_{st} + 0.5736) \quad (36)$$

Resistance voltage loss is the voltage drop due to ohmic resistance, which comprises electrolyte resistance and the hydrogen ion transportation resistance through Nafion. It can be shown as the expression below [4].

$$v_{ohm} = i \cdot R_{ohm} \quad (37)$$

$$R_{ohm} = \frac{t_m}{\sigma_m} \quad (38)$$

$$\sigma_m = (b_1\lambda_m - b_2)\exp\left(1268\left(\frac{1}{303} - \frac{1}{T_{st}} \right) \right) \quad (39)$$

where b_1 and b_2 are decided according to the membrane specification (Nafion117).

The formation of concentration voltage loss is generated because the oxygen and nitrogen inside the stack cannot be delivered by constant pressure due to flow resistance. Therefore, it can be represented by the loss of the chemical reaction [9].

$$v_{conc} = c_2 i^{(1+c_3)} \quad (40)$$

According to the experimental results, the two constants of c_2, c_3 can be accurately estimated.

Table1. Parameters used in the simulation [9].

Parameters	value
$A_{fc}\,(\text{m}^2)$	100×10^{-4}
N	46
$t_m\,(\text{m})$	35×10^{-6}
$\rho_{memb,dry}\,(\text{kg/m}^3)$	2×10^3
$M_{menb,dry}\,(\text{kg/mol})$	1.1
$K_{ca,out}\,(\text{kg/(bar}\cdot\text{s}))$	0.01
$K_{an,out}\,(\text{kg/(bar}\cdot\text{s}))$	0.001
$V_c\,,V_{an}\,(\text{m}^3)$	7.59×10^{-4}
$t_{puge}\,(\text{s})$	0.5
ε	0.5
$D_v\,(\text{m}^2/\text{s})$	34.5×10^{-6}
$\delta_{GDL}\,(\text{m})$	0.05×10^{-3}
$\gamma\,(\text{s}^{-1})$	0.9×10^3
s_{im}	0.1
$s_{ca}\,,s_{ca}$	0.18
$\mu\,(\text{m}^2)$	120
$\eta_l\,(\text{kg/(m}\cdot\text{s}))$	978
$|dp_c/ds|\,(\text{pa})$	30321
c_1	15
c_2	288.59
c_3	14
b_1	0.005139
b_2	0.00326
α_f	0.5
α_p	0.5

2.5 Cathode GDL model

2.5.1 Gas model

Using the ideal gas state equation, the following equations are obtained:

$$c_{v,caGDL} = \frac{P_{v,caGDL}}{RT_{st}} \tag{41}$$

$$c_{v,ca} = \frac{P_{v,ca}}{RT_{st}} \tag{42}$$

The effective diffusion coefficient can be obtained as [7]

$$\langle D_{v,ca}\rangle = D_v\varepsilon\left(\frac{\varepsilon - 0.11}{1 - 0.11}\right)^{0.785}\left(1 - s_{ca}\right)^2 \tag{43}$$

where

$$s_{ca} = \frac{V_{l,ca}}{V_p} \tag{44}$$

The mole flow rate can be obtained from the effective diffusion coefficient and mole concentration as

$$N_{v,ca} = -\langle D_{v,ca}\rangle\left(\frac{c_{v,ca} - c_{v,caGDL}}{\delta GDL}\right) \tag{45}$$

The water steam partial pressure inside the diffusion layers is evaluated as

$$\frac{dP_{v,caGDL}}{dt} = RT_{st}\left(\frac{N_{v,gen} + N_{v,memb} - N_{v,ca}}{\delta GDL} + R_{ca,evap}\right) \tag{46}$$

where

$$R_{ca,evap} = \gamma\frac{P_{sat}(T_{sat}) - P_{v,caGDL}}{RT_{st}} \tag{47}$$

The number of activated oxygen and produced water content can be calculated from the electrochemical relation as

$$N_{O_2,react} = \frac{I_{st}}{4FA_{fc}} \tag{48}$$

$$N_{v,gen} = \frac{I_{st}}{2FA_{fc}} \tag{49}$$

The mass flow rate between GDL and cathode channel can be described as

$$W_{O_2,caGDL} = A_{fc}nM_{O_2}N_{O_2,react} \tag{50}$$

$$W_{v,caGDL} = A_{fc}nM_vN_{v,ca} \tag{51}$$

2.5.2 Liquid model

Using the mass balance equation, the following equation can be obtained. The mass flow rate from capillary phenomenon can be obtained as

$$\rho_l\frac{dV_{l,caGDL}}{dt} = -W_{l,caGDL} - R_{ca,evap}M_v\varepsilon V_{GDL} \tag{52}$$

The liquid water mass flow rate at the capillary of GDL can be expressed as [22]

$$W_{l,caGDL} = \frac{A_{fc}n_{fc}\mu\mu_{rl}}{\eta_l}\left|\frac{d\rho_c}{dS}\right|\frac{S_{ca}}{\delta GDL} \tag{53}$$

where

$$S_{ca} = \begin{cases} \dfrac{s_{ca} - s_{im}}{1 - s_{im}}; & s_{im} < s_{ca} \leq 1 \\ 0\,; & 0 \leq s_{ca} \leq s_{im} \end{cases}$$

$$\mu_{rl} = S_{ca}^3 \tag{54}$$

2.6 Anode GDL model

As the anode GDL model is very similar to the cathode GDL model, only the mass balance equation is described as

$$\frac{dP_{v,anGDL}}{dt} = RT_{st}\left(\frac{N_{v,an} - N_{v,memb}}{\delta GDL} + R_{an,evap}\right) \qquad (55)$$

3. Model calibration

In this study, experiments are performed to calibrate the dynamic fuel cell model describing the Ballard Nexa. The model was utilized to control the stack

Fig. 2. Experimental set of the PEMFC system.

operation accurately, which is comprised of fuel cell stacks and a control module. The control module is comprised of three parts: first is the chemical reaction control part of oxygen, nitrogen, and their pressures; second is the purge solenoid valve control that extracts the water by-product; and third is the cooling fan control that regulates the stack temperature. The rated power for the fuel cell is 1.2KW, while its operating voltage has a wide range, from 22 to 50 V. The starting voltage comes from the battery, and the fuel cell load is supplied using the 1000W DC electric load of a Unicorn-Tmi. Fig. 2 shows the experimental setup, while Fig. 3 represents the mathematical modeling using Matlab/Simulink. Through the model and experimental setup, we measured the stack current, for its merit of easy obtainability, and voltage, which gives a good presentation of the fuel cell.

In Fig. 3, W_{cain1} and W_{anin1} are the blocks used to calculate the mass flow going into the cathode and anode, respectively. They are represented by Eq. 56 to Eq. 64 below.

In this research, the temperature and pressure of the inputs of anode and cathode are set to a normal state, while the relative humidity of each input is set to zero. The mass flow rate of the cathode input and the compressor output were obtained as follows:

Fig. 3. PEMFC model in Matlab/Simulink.

$$W_{O_2,com,out} = \frac{I_{st}}{4F} M_{O_2} n \lambda_{ca} \tag{56}$$

$$W_{a,com,out} = \frac{W_{O_2,com,out}}{x_{O_2,com,out}} \tag{57}$$

$$W_{N_2,com,out} = W_{a,com,out} - W_{O_2,com,out} \tag{58}$$

Each component's mass flow rate to the membrane via a humidifier is calculated as

$$P_{v,ca,in} = \phi_{ca,in} P_{sat} \tag{59}$$

$$W_{a,ca,in} = W_{a,com,out} \tag{60}$$

$$W_{v,ca,in} = M_{H_2O} \frac{W_{a,ca,in} P_{v,ca,in}}{M_a (P_{ca,in} - P_{v,ca,in})} \tag{61}$$

$$W_{O_2,ca,in} = W_{O_2,com,out} \tag{62}$$

$$W_{N_2,ca,in} = W_{N_2,com,out} \tag{63}$$

As the relative humidity at the anode input is zero, only the mass flow rate of hydrogen is required as

$$W_{H_2,an,in} = \frac{I_{st}}{2F} M_{H_2} n \lambda_{an} \tag{64}$$

The stack voltage, which usually represents the characteristics of fuel cell well, is used as the measuring parameter. As represented in Figs. 4 and 5, the simulation and experimental results of the fuel cell with air and hydrogen have a 2.5 and 1.3 excess ratio, a relative humidity of 0.8 at the cathode input, and a stack temperature of 60°C. Cell average voltage as well as constant pressure and temperature inside the stack were assumed. Modeling of the fuel cell stack has been well presented, as shown in both figures.

4. Optimization design using RSM

In this paper, maximum power and minimum hydrogen consumption under a certain power range are selected as the objective function. Maximum power without any external constraints provides the fuel cell output characteristics. It is necessary to obtain the minimum hydrogen consumption with power constraints for real fuel cell application. To obtain the optimized conditions for maximum power and minimum hydrogen consumption under a certain power range, optimization is carried out using RSM based on the dynamic PEMFC model. Optimal design using RSM can reduce the optimization time and computa-
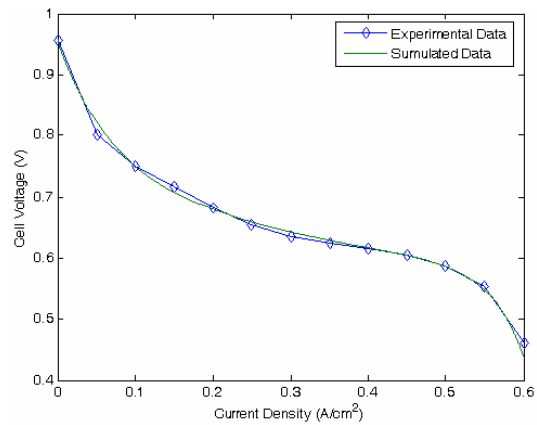

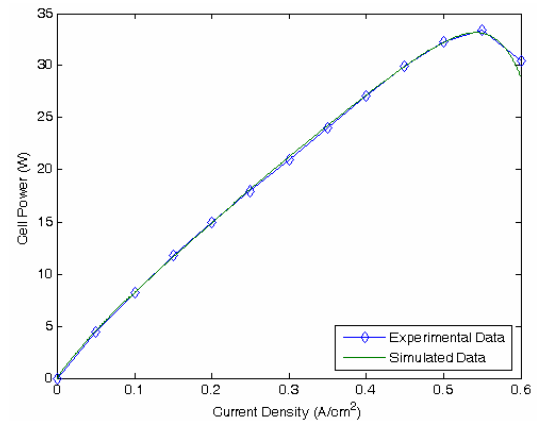Fig. 4. I-V Characteristic curve comparison.

Fig. 5. I-P Characteristic curve comparison.

tional effort compared with optimal design using PEMFC stack model directly. The stack current, stack temperature, oxygen excess ratio, hydrogen excess ratio, and inlet air humidity are chosen as the varying parameters to study the interrelated response, as well as to perform the optimization using these variables, because the other factors do not have critical influences for the optimization. Table 2 shows the minimum, average, and maximum values of each parameter, which are converted into the non-dimensional parameters of -1, 0, and 1, respectively.

4.1 Response surface methodology

RSM is a statistical analysis method used for a response surface made from the change of each variable. The changes in the design variables have a complex interrelated reaction chain. These design variables represent the independent parameter or factor that affects the system response, while the response vari-

Table 2. Lower and upper bound of each design variable and their non-dimensionlization.

Design Variable	Minimum Value	Middle Value	Maximum Value
I_{st} (A)	36(-1)	43(0)	50(1)
T_{st} (℃)	55(-1)	60(0)	65(1)
$\lambda_{ca,in}$	1.5(-1)	2.5(0)	3.5(1)
$\lambda_{an,in}$	1.1(-1)	1.3(0)	1.5(1)
$\Phi_{ca,in}$	0.6(-1)	0.8(0)	1(1)

ables represent the dependent ones that affect a certain response due to the reaction of the design variables.

In this paper, response surface was composed of quadratic order polynomial as shown in Eq. 65. The equation represents a simple and smooth curved surface with minimal numerical error.

$$C_m(x_i) = c_0 + \sum_{i=1}^{k} c_i x_i + \sum_{i=1}^{k} c_{ii} x_i^2 + \sum_{i=1}^{k-1} \sum_{j=2(j>i)}^{k} c_{ij} x_i x_j \quad (65)$$

where $C_m(x)$ represents the response variable, x_i is the design variable, c_i is the undetermined polynomial coefficient, and k represents the number of design variables. When the response model is defined as a quadratic order polynomial, the number of coefficients p can be expressed as $(k+1)(k+2)/2$.

The D-optimality method is used to select experimental points for constructing the response surface, which is one of the Design of Experiments (DOE) methods [23]. The D-optimality method chooses the experimental points that can minimize the response of uncertain model parameters and the maximum variance of the response values.

4.2 Construction of response surface

In this study, optimization is performed using the dynamic fuel cell model in order to improve the confidence of response surface. According to Table 3, 42 experimental points are selected using the D-optimality method, which are twice as many as the undetermined parameters. The undetermined coefficients of c_i are calculated as shown in Table 4. The evaluation index for response surface reliability R_{adj}^2 is 0.997, which shows near perfect reliability.

4.3 Optimal design with the obtained response surface

As the balance of plant (BOP) used in our system

Table 3. Analysis results of the selected experimental points.

No.	I_{st}	T_{st}	λ_{ca}	λ_{an}	$\Phi_{ca,in}$	Power(W)
1	1	-1	1	-1	-1	1207.05
2	0	1	1	-1	0	1346.87
3	-1	-1	0	-1	1	916.53
4	-1	1	1	0	1	1139.25
5	-1	1	-1	-1	1	970.42
6	1	1	0	-1	-1	1456.03
7	1	-1	1	-1	1	1235.27
8	-1	0	-1	0	1	946.01
9	1	-1	-1	-1	0	963.18
10	1	1	-1	0	-1	1283.49
11	-1	1	1	1	-1	1139.51
12	-1	1	-1	1	-1	971.48
13	-1	-1	1	-1	-1	963.23
14	1	0	1	0	0	1476.58
15	1	-1	-1	0	1	961.35
16	-1	1	1	-1	-1	1138.45
17	1	-1	-1	1	-1	940.76
18	-1	-1	1	1	0	962.54
19	1	1	-1	1	0	1284.45
20	1	-1	0	1	1	1125.08
21	0	0	0	0	0	1224.06
22	1	1	1	1	-1	1547.25
23	0	0	0	1	-1	1217.14
24	-1	-1	0	0	-1	904.61
25	1	-1	1	1	-1	1190.15
26	-1	0	1	-1	1	1108.40
27	-1	1	0	1	1	1081.18
28	-1	-1	1	1	1	967.97
29	0	-1	1	0	1	1109.11
30	1	1	-1	-1	1	1282.46
31	-1	-1	-1	1	1	801.84
32	1	0	-1	-1	-1	1224.06
33	-1	0	1	1	-1	1098.70
34	0	-1	-1	-1	1	900.14
35	1	0	-1	1	1	1220.80
36	0	1	-1	1	1	1133.39
37	-1	-1	-1	-1	0	805.23
38	1	1	1	1	1	1547.24
39	1	1	1	-1	1	1545.25
40	0	-1	-1	-1	-1	892.13
41	-1	-1	-1	1	-1	797.05
42	-1	1	-1	-1	-1	970.42

consumes the energy from PEMFC, the BOP energy consumption should be considered in the optimization process. The maximum consumed energy of BOP is obtained in the experiment as

Table 4. Coefficients for the constructed response surface of power.

No.	Coefficients	No.	Coefficients
1	0.122668E+04	12	0.398440E+02
2	0.144727E+03	13	0.241861E+02
3	0.125200E+03	14	-0.150474E+01
4	0.104815E+03	15	0.223453E+01
5	0.249083E+01	16	0.154030E+01
6	0.280986E+01	17	0.221570E+01
7	0.810278E+01	18	-0.485575E+01
8	0.776208E+02	19	0.787513E+00
9	0.302343E+02	20	0.231916E+01
10	0.824385E+00	21	0.434485E+01
11	0.200230E+01		

Table 5. Description of optimization cases.

Item	Objective	Constraint
Opt. 1	Maximize Power	No
Opt. 2	Minimize Mass Flow Rate of Hydrogen	Power =800~1225

$$P_{para,\max} = -4.67 \times 10^{-6} I_{st}^5 + 5.57 \times 10^{-4} I_{st}^4 \\ - 0.02248 I_{st}^3 + 0.3305 I_{st}^2 + 2.7879 I_{st} + 36.0686 \tag{66}$$

Table 6. Optimal results of each case.

Case	I_{st} (A)	T_{st} (°C)	λ_{ca}	λ_{an}	$\Phi_{ca,in}$	Power (W)	W_{H2} (kg/s)
Baseline	36	55	1.5	1.1	0.6	678.5	2.88e-5
Opt. 1	50	64.87	3.5	1.5	1.00	1229.7	4.65e-5

The BOP power consumption is mainly related with two power demands. One is from the air pump and the other is from the cooling fan. The actual BOP energy consumption can be represented using the weighting factor of air pump and cooling fan, α_p, α_f, respectively, as

$$P_{para} = \alpha_p P_{para,\max} \frac{\lambda_{ca}}{3.5} + \alpha_f P_{para,\max} \frac{T_{st}}{3.5} \tag{67}$$

In this research, as represented in Table 5, the optimization using RSM is performed by changing the objective function and constraint in consideration of the BOP energy consumption, and SQP is used as the optimization algorithm.

As shown in Table 6, the maximum PEMFC total power can be obtained by changing the operating variables of stack current, temperature, oxygen and hydrogen excess ratio, and cathode input humidity
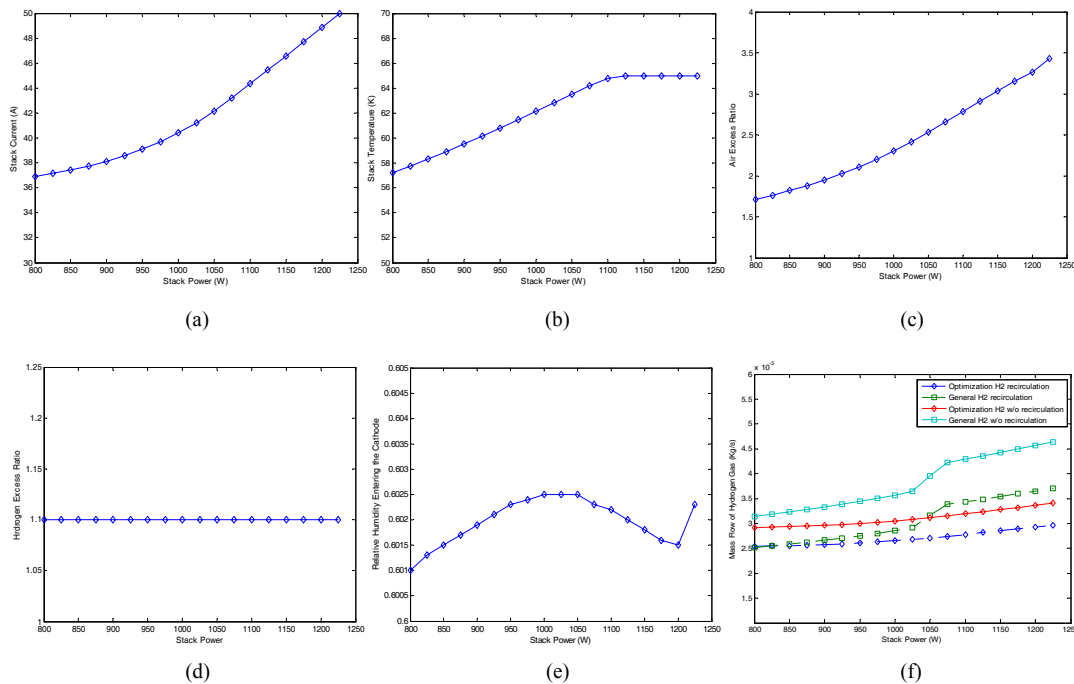

Fig. 6. Minimizing mass flow rate of hydrogen.

while increasing hydrogen consumption.

Figs. 6(a) to 6(e) show the results of stack current, temperature, oxygen and hydrogen excess ratio, and cathode input humidity by rendering the hydrogen consumption to a minimum, respectively. The rated PEMFC power ranges from 800 to 1225 W. Figure 6f shows the comparison of hydrogen consumption between the optimized one and the general one, in which the design variables for the general one is presented by the middle values as shown in Table 2. Moreover, the figure shows the consumed hydrogen with recirculation and without recirculation. From this figure, it is suggested that the hydrogen consumption can be minimized especially at a higher power region, where the fuel consumption can be minimized to almost 50 percent without recirculation. In the case of recirculation, hydrogen consumption can be decreased even more. As the hydrogen price keeps increasing, this optimal energy consumption technique is facing the challenge and improving its effectiveness for future PEMFC vehicle operation. Furthermore, the optimization process with RSM has the advantage of obtaining optimal operating conditions effectively under certain constrained operating conditions.

5. Conclusion

In this paper, the stack voltage model, mass flow model, membrane hydration model, and two GDL models are introduced to create the dynamic PEMFC model. By comparing with the experimental results, the proposed dynamic model was calibrated. Based on the calibrated mathematical fuel cell model, the stack current, stack temperature, air excess ratio, hydrogen excess ratio, and inlet air humidity were chosen as the design variables to obtain the generalized stack power considering BOP. The SQP algorithm along with the RSM was applied to obtain the optimized design parameters corresponding to the maximum power. Moreover, minimal hydrogen consumption optimization can also be performed under certain power ranges. The introduced dynamic PEMFC model of this study may provide a useful tool in designing and analyzing PEMFC, and the optimization process can be fully applied as an efficient tool to construct important fuel cell vehicle control strategy.

Nomenclature───────────────────

a	:	Water activity
A_{fc}	:	Fuel cell active area, m^2
c	:	Mole concentration, mol/m^3
D	:	Diffusion coefficient, m^2/sec
$<D>$	:	Effective diffusion coefficient, m^2/sec
E	:	Fuel cell open circuit voltage, V
F	:	Faraday constant, C /mol
i	:	Current density, A/cm^2
I	:	Stack current, A
K	:	Valve coefficient, kg/(bar·s)
m	:	Mass, kg
M	:	Molecular mass, kg/mol
n	:	Number of cells
n_d	:	Electro-osmotic drag coefficient
N	:	Molar flux, mol/(s·m^2)
P	:	Pressure or power, pa or w
R	:	Gas constant or electrical resistance, Ω
s	:	Fraction of liquid water volume to the total volume
s_{im}	:	Level of immobile saturation
S	:	Reduced liquid water saturation
t	:	Time, s
t_m	:	Membrane thickness, cm
T	:	Temperature, K
V	:	Volume or voltage, m^3 or V
W	:	Mass flow rate, kg/s
x	:	Mass fraction
y	:	Mole fraction

Greek symbols

γ	:	Volumetric condensation coefficient, s^{-1}
δ	:	Thickness of diffusion layer, m
ε	:	Porosity or emissivity
η	:	Viscosity, kg/(m·s)
λ	:	Water content or excess ratio
μ	:	Permeability, m^2
μ_r	:	Relative permeability, kg/mol
ρ	:	Mass density, kg/m^3
σ_m	:	Membrane conductivity
Φ	:	Relative humidity
ω	:	Humidity ratio

Subscripts

a	:	Dry air
act	:	Activation loss
an	:	Anode
atm	:	Atmospheric
c	:	Capillary
ca	:	Cathode

com	:	Compressor
conc	:	Concentration loss
dry	:	Dry
evap	:	Evaporation
fc	:	Fuel cell
gen	:	Generated
GDL	:	Gas diffusion layer
H_2	:	Hydrogen
H_2O	:	Water
in	:	Inlet
l	:	Liquid water
m	:	Membrane
max	:	Maximum
memb	:	Across membrane
N_2	:	Nitrogen
ohm	:	Ohmic loss
out	:	Outlet
O_2	:	Oxygen
para	:	Parasitic

References

[1] J. H. Bang, H. S. Kim, D. H. Lee and K. D. Min, Study on operating characteristics of fuel cell powered electric vehicle with different air feeding systems, *Journal of Mechanical Science and Technology*, 22 (2008) 1602-1611.

[2] M. W. Verbrugge and R. F. Hill, Ion and solvent transport in ion-exchange membrane, *J. Eletrochemical Society*, 137 (3) (1990) 893-899.

[3] D. M. Bernardi and M. W. Verbrugge, A Mathematical model of the solid polymer-electrolyte fuel cell, *Journal of the Electrochemical Society*, 139 (9) (1992) 2477-2491.

[4] T. E. Springer, T. A. Zawodzinski and S. Gottesfeld, Polymer electrolyte fuel cell model, *Journal of Electrochemical Society*, 138 (8) (1991) 2334-2342.

[5] G. Sylvain, A. G. Stephanopoulos, et al., Dynamics of low-pressure and high-pressure fuel cell air supply systems, *Proceedings of the American Control Conference*, (2003) 2049-2054.

[6] J. T. Pukrushpan, H. Peng and A. G. Stefanopoulou, Control-oriented modeling and analysis for automotive fuel cell Systems, *Journal of Dynamic Systems, Measurement, and Control*, 126 (1) (2004) 14-25.

[7] J. H. Nam and M. Kaciany, Effective diffusivity and water-saturation distribution in single-and two-layer PEMFC diffusion medium, *International Journal of Heat and Mass Transfer*, 46 (24) (2003) 4595-4611.

[8] D. A. Mckay, W. T. Ott and A. G. Stefanopoulou, Modeling, parameter identification, and validation of reactant and water dynamics for a fuel cell stack, *Proceedings of IEMCE'05*, IMECE2005-81484.

[9] A. J. del Real, A. Arce and C. Bordons, Development and experimental validation of a PEM fuel cell dynamic model, *J. of Power Sources*, 173 (1) (2007) 310-324.

[10] S. K. Park and S. Y. Choe, Dynamic modeling and analysis of a 20-cell PEM fuel cell stack considering temperature and two-phase effects, *J. of Power Sources*, 179 (2008) 660-672.

[11] C. Park, K. Oh, D. Kim and H. Kim, Development of fuel cell hybrid electric vehicle performance simulator, *International Journal of Automotive*, 5 (4) (2004) 287-295.

[12] M. J. Kim and H. Peng, Power management and design optimization of fuel cell/battery hybrid vehicles, *J. of Power Sources*, 165 (2007) 819-832.

[13] G. Sikha and B. N. Popov, Performance optimization of a battery-capacitor hybrid system, *J. of Power Sources*. 134 (2004) 130-138.

[14] H. H. Lin, C. H. Cheng, C. Y. Song, F. Chen and W. M. Yan, Optimization of key parameters in the proton exchange membrane fuel cell, *J. of Power Sources*, 162 (2006) 246-254.

[15] G. E. P. Box and K. B. Wilson, On the experimental attainment of optimum conditions, *Journal of the Royal Statistical Society, Series B*, 13 (1) (1951) 1-45.

[16] W. J. Rox, N. Stander and R. T. Haftka, Response surface approximations for structural optimization, *International Journal for Numerical Methods in Engineering*, 42 (3) (1998) 517-534.

[17] Z. Z. Li, Y. D. Shen, H. L. Xu, J. W. Lee, K. S. Heo and S. Y. Seol, Optimal design of high temperature vacuum furnace using response surface method, *Journal of Mechanical Science and Technology*, 22 (11) (2008) 2213-2217.

[18] P. E. Gill, W. Murray and M. H. Wright, *Practical Optimization, Academic Press*, London and New York, (1981).

[19] T. V. Nguyen and R. E. White, A water and heat management model for proton-exchange-membrane fuel cells, *Journal of Electrochemical Society*, 140 (8) (1993) 2178-2186.

[20] S. Dutta, S. Shimpalee and J. W. Van Zee, Numerical prediction of mass-exchange between cathode and anode channels in a PEM fuel cell, *International Journal of Heat and Mass Transfer*, 44

(2001) 2029-2042.

[21] J. C. Amphlett, R. M. Baumert, R. F. Mann, et al., Performance modeling of the ballard mark IV solid polymer electrolyte fuel cell, *Journal of the Electrochemical Society*, 142 (1) (1995) 9-15.

[22] M. Kaviany, *Principles of Heat Transfer in Porous Media*, 2nd ed., Springer, (1999).

[23] M. J. Box and N. R. Draper, Factorial designs, the |XTX| criterion and some related matters, *Technometrics*, 13 (4) (1971) 731-742.

Dong-Ji Xuan received his B.S. degree in Mechanical Engineering from Harbin Engineering University, China in 2000. He then received his M.S. degree in Mechanical Engineering from Chonnam National University, South Korea in 2006. Currently, he is a Ph.D. candidate of the Department of Mechanical Engineering, Chonnam National University, South Korea. His research interests include control and optimization of PEM fuel cell system, dynamics and control, and mechatronics.

Zhen-Zhe Li received his B.S. degree in Mechanical Engineering from Yanbian University, China in 2002. He then received his M.S. degree in Aerospace Engineering from Konkuk University, South Korea in 2005 and his Ph.D. degree in Mechanical Engineering from Chonnam National University, South Korea in 2009. Dr. Li is currently a Researcher of the Department of Mechanical Engineering in Chonnam National University, South Korea. Dr. Li's research interests include applied heat transfer, fluid mechanics, and optimal design of thermal and fluid systems.

Jin-Wan Kim received his B.S. degree in Aerospace Engineering from Chosun University, South Korea in 1990. He then received his M.S. degree in Aerospace and Mechanical Engineering from Korea Aerospace University, South Korea in 2003 and his Ph.D degree in Mechanical Engineering from Chonnam National University, South Korea in 2008. He is currently a Post Doctor of the Department of Mechanical Engineering in Chonnam National University, South Korea. His research interests include control of hydraulic systems, dynamics and control, and mechatronics.

Young-Bae Kim received his B.S. degree in Mechanical Design from Seoul National University, South Korea in 1980. He then received his M.S. degree in Mechanical Engineering from the Korean Advanced Institute of Science and Technology (KAIST), South Korea in 1982 and his Ph.D. degree in Mechanical Engineering from Texas A&M University, USA in 1990. Dr. Kim is currently a Professor of the School of Mechanical and Systems Engineering in Chonnam National University, South Korea. Dr. Kim's research interests include mechatronics, dynamics and control, and fuel cell hybrid electric vehicle (FCHEV) systems.